Fe nanocrystal growth on $SrTiO_3(001)$

Fabien Silly and Martin R. Castell[a)]
Department of Materials, University of Oxford, Parks Road, Oxford OX1 3PH, United Kingdom

(Received 7 April 2005; accepted 20 June 2005; published online 1 August 2005)

We have investigated the structure and morphology of self-assembled iron nanocrystals supported on a $SrTiO_3(001)$-$c(4\times2)$ substrate using scanning tunneling microscopy. Nanocrystals with a truncated pyramid shape were imaged, which result from the epitaxial growth of bcc Fe on $SrTiO_3(001)$. By using the dimensions of the nanocrystal facets at equilibrium and an energy minimization calculation, we obtain the adhesion energy $\gamma_{adh}=(3.05\pm0.15)$ J/m^2 for bcc Fe on $SrTiO_3(001)$-$c(4\times2)$. © *2005 American Institute of Physics*. [DOI: 10.1063/1.2008375]

Magnetic materials composed of densely packed nanocrystals are of interest because they exhibit different magnetic properties compared to the bulk solids. For example, such materials can show different magnetization directions, have enhanced magnetic moments, or display lower Curie temperatures. Organized arrays of self-assembled magnetic nanocrystals also have possible applications in the area of high-density information storage media. Iron in the bcc structure is of particular interest because of its high magnetic moment and remnant magnetization. However, if iron is grown in ultrathin film form it often adopts the fcc structure,[1–5] where a small variation of the lattice constant or lattice distortion can result in drastic changes of magnetic phases including a low-moment ferromagnetic phase, an antiferromagnetic phase, a ferrimagnetic phase, and high-moment ferromagnetic phases. A description of the properties of nanocrystalline Fe therefore requires knowledge of the structure, size, shape, and distribution of the nanocrystals.

In this letter we report on the epitaxial growth of Fe nanocrystals on a $SrTiO_3(001)$ substrate. Fe self-assembles into truncated pyramid nanocrystal domains. A precise analysis of the pyramidal cluster shape shows that Fe is bcc packed. The equilibrium nanocrystal shape is used to determine the adhesion energy of bcc Fe on $SrTiO_3$.

Interest in the $SrTiO_3$ surface has emerged from its electronic properties[6] and its use as a substrate for supported nanocrystal growth.[7] The $SrTiO_3(001)$ surface presents a multitude of different reconstructions[8,9] depending on sample preparation, which can be used for the growth of regular nanocrystals over macroscopic length scales. $SrTiO_3$ crystallizes into the cubic perovskite structure with a 3.905 Å lattice parameter. In its pure form it has a 3.2 eV band gap that would make it unsuitable for imaging in the scanning tunneling microscope (STM). To overcome this problem we use crystals doped with 0.5% (weight) Nb. The crystals were epipolished (001) and supplied by PI-KEM, UK. We deposited Fe from an *e*-beam evaporator (Oxford Applied Research EGN4) using 99.99% pure Fe rods supplied by Goodfellow, UK. Our STM is manufactured by JEOL (JSTM 4500xt) and operates in ultrahigh vacuum (10^{-8} Pa). We used etched Pt/Ir tips to image the samples at room temperature and elevated temperatures, with a bias voltage applied to the sample. $SrTiO_3(001)$-$c(4\times2)$ reconstructed surfaces were obtained after 10 min of Ar^+ bombardment at 500 eV and a subsequent anneal in UHV between 900 and 1050 °C for up to 1 h.

Figure 1 shows the $SrTiO_3(001)$-$c(4\times2)$ surface. This surface is characterized by its straight step edges that run along the ⟨100⟩ directions.[8] This surface is also a precursor for nanoline growth on $SrTiO_3(001)$.[10] The $c(4\times2)$ reconstruction was verified by low-energy electron diffraction (LEED).

Figure 2 shows an STM image of the $SrTiO_3(001)$-$c(4\times2)$ surface after room-temperature Fe deposition and a 10-min anneal at 360 °C. Self-assembled Fe nanocrystals cover the surface. The Fe nanocrystals are randomly distributed and there is no preferential nucleation on the substrate step edges. The sample was then annealed at 300 °C for 10 h in UHV. This treatment causes some ripening of the nanocrystals and allows individual nanocrystals to attain their equilibrium shapes as shown in Fig. 3. The STM image in Figs. 3(a) and 3(b) shows that Fe has self-assembled into similarly sized nanocrystals. The Fe nanocrystals have a square top surface and a square base, resulting in the shape of a truncated four-sided pyramid. Only this shape of nanocrystal was observed. The predominant cluster height was measured to be 18.55 Å. Nanocrystal heights are quantized into steps of

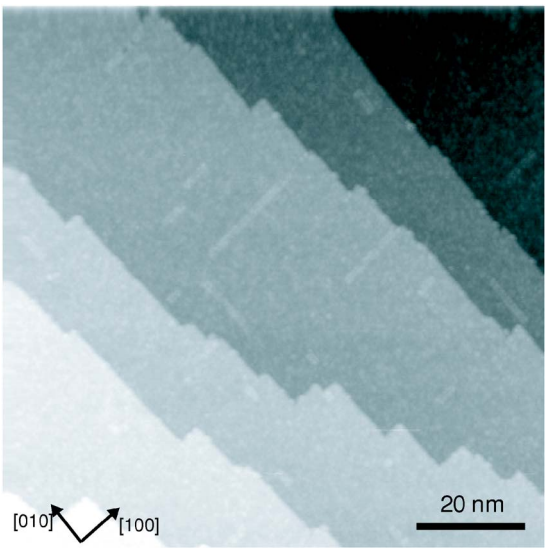

FIG. 1. (Color online) $SrTiO_3(001)$ after Ar^+ bombardment and a 10-min 1050 °C UHV anneal. This results in a $c(4\times2)$ reconstructed surface with straight step edges and unit cell (3.9 Å) step heights. Image size: 100×100 nm^2; sample bias: $V_s=+1.5$ V; tunneling current: $I_t=0.1$ nA.

a)Electronic mail: martin.castell@materials.oxford.ac.uk

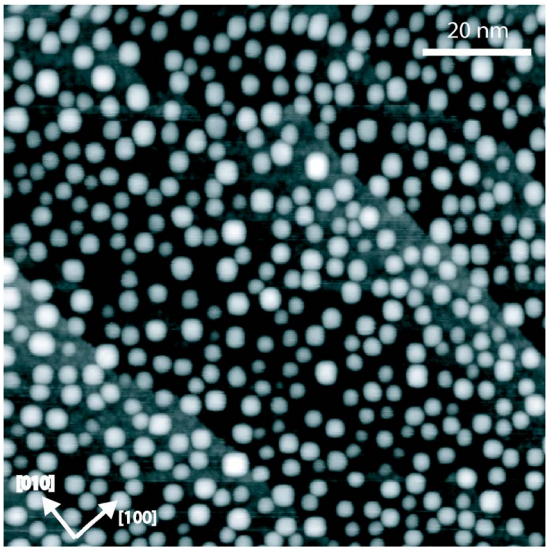

FIG. 2. (Color online) Fe deposition onto a room-temperature $SrTiO_3(001)$-$c(4\times2)$ substrate followed by an anneal of 360 °C for 10 min gives rise to self-assembled Fe nanocrystals. Image size: 100×100 nm^2; sample bias: $V_s=+1.0$ V; tunneling current: $I_t=0.1$ nA.

1.4 Å as shown in the histogram in Fig. 3(c). The ratio of the length (ℓ) of the top square to the height (h) of the truncated pyramids as a function of volume is shown in Fig. 3(d). The constant ratio of $\ell/h=1.20\pm0.12$ implies that these pyramidal nanocrystals have reached their equilibrium shape. The error in the ratio denotes the standard deviation of the measurements. The angle α between opposing side facets of the nanocrystals was measured to be $90.8°\pm1.2°$ [Figs. 3(e) and 3(f)]. As a guide to the eye we have shown in Fig. 3(g) a schematic illustration of a truncated pyramid. We did not observe any shape transitions with volume or temperature as observed in the case of $Pd/SrTiO_3(001)$,[7] or in strained Ge on Si growth.[11,12]

The STM images show that iron forms truncated pyramid nanocrystals on $SrTiO_3(001)$. This crystal shape can only evolve from cubic packing. Cubic-packed Fe thin films can exist in the fcc and bcc structures. The equilibrium truncated pyramid shape for the fcc structure has a (001) top facet and four (111) side facets, these being the lowest energy facets. On the other hand, in the bcc structure the lowest energy facets are the (001) and the (011) facets.[13] This means that the equilibrium truncated pyramid shape for the bcc structure has a (001) top facet and four (011) side facets.

A truncated pyramid-shaped fcc Fe nanocrystal will have (111) side facets that have an angle of 54.7° with respect to the substrate and an angle of 70.6° between each other. The unit cell dimension for fcc Fe is $a_{fcc}\approx3.6$ Å, and as the interplanar periodicity along the [001] direction is half the unit cell dimension, we would expect fcc nanocrystals to be quantized in heights of ~1.8 Å. However, if the Fe nanocrystals have bcc packing, their shapes are subtly different. The (011) side facets have a 45° angle with respect to the substrate and a 90° angle between each other. The unit cell dimension for bcc Fe is $a_{bcc}=2.87$ Å and the height quantization is therefore ~1.44 Å. Our data show that the measured side facets angle is $90.8°\pm1.2°$ [Figs. 3(e) and 3(f)] and that the islands are quantized into heights of 1.4 Å multiples [Fig. 3(c)]. We therefore conclude that the truncated pyramid nanocrystals reported on here have a bcc structure.

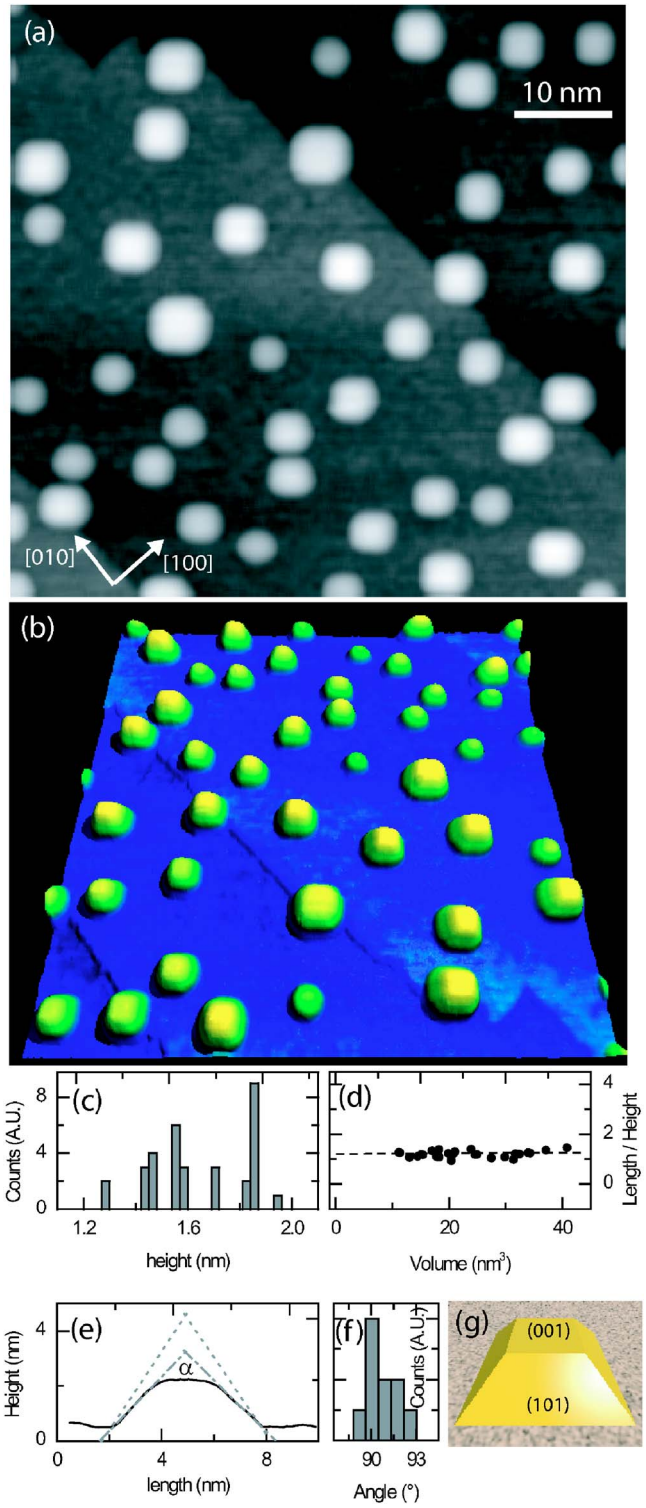

FIG. 3. (Color online) STM image (a) and 3D representation (b) of truncated pyramid-shaped Fe nanocrystals on a $SrTiO_3(001)$-$c(4\times2)$ substrate. A 300 °C anneal for 10 h allows the nanocrystals to reach their equilibrium shape. Image size: 67×63 nm^2; sample bias: $V_s=+1.0$ V; tunnelling current: $I_t=0.1$ nA. (c) A pyramid height histogram showing quantization of the heights into steps of ~1.4 Å. (d) The length-to-height ratio of the nanocrystals is constant with volume at $\ell/h=1.20\pm0.12$. (e) A profile taken through a pyramid (solid line). The dash dot line shows a 90° angle and the dotted line shows a 70.6 ° angle for comparison. (f) A histogram of the measured facet angles α of the pyramid nanocrystals. (g) A schematic model of a bcc Fe pyramid.

Our STM images show that the low index axes of the Fe nanocrystals are rotated by 45° with respect to the $SrTiO_3(001)$ substrate. The interface crystallography is

therefore $(001)_{Fe}\|(001)_{SrTiO_3}$, $[100]_{Fe}\|[110]_{SrTiO_3}$. The necessity of the 45° rotation can be justified by a lattice matching argument. The $SrTiO_3$ unit cell dimension along the [110] direction is 5.52 Å. Two Fe unit cells along the [100] direction have a value of 5.74 Å. A small compressive lattice mismatch of 4% and a commensurate interface can therefore be achieved via the 45° rotation. The largest nanocrystals we have imaged have a base width of around 6 nm, which is below the limit where misfit dislocations are required (7.2 nm), and the lattice mismatch is therefore presumably wholly taken up by elastic strain. No other type of dislocations due to anomalies in growth, such as screw dislocations, were imaged by the STM.

The equilibrium shape of an iron nanocrystal on a $SrTiO_3(001)$ substrate is determined by the surface energies of the Fe crystal facets (γ_{hkl}), the interface energy between the Fe crystal and the substrate (γ_i), and the surface energy of the substrate (γ_{STO}). In our case only {101} and {001} facets are seen on the nanocrystals and therefore the change in surface and interface energy between a bare substrate and one supporting a crystal is

$$E = \gamma_{001}A_{001} + \gamma_{101}A_{101} + \gamma_i A_i - \gamma_{STO}A_i = \gamma_{001}A_{001} + \gamma_{101}A_{101} + \gamma^* A_i, \quad (1)$$

where A_{001} and A_{111} are the Fe facet areas, A_i is the interface area, and γ^* is defined as $\gamma_i - \gamma_{STO}$.[14] For a supported crystal of a given volume to find its equilibrium shape E will be at a minimum. Straightforward analysis via the modified Wulff construction[14] or by minimizing E analytically results in the following equation for γ^* for the truncated pyramid shape as a function of γ_{001}, γ_{101}, and the length-to-height ratio.

$$\gamma^* = 2\frac{h}{\ell}(\sqrt{2}\gamma_{101} - \gamma_{001}) - \gamma_{001}. \quad (2)$$

In this equation we can substitute the ℓ/h ratio from our experiments, and use the theoretically calculated bcc Fe surface energies of Spencer *et al.*[13] ($\gamma_{001}=2.29$ J/m^2, $\gamma_{110}=2.27$ J/m^2), which results in $\gamma^*=(-0.76\pm0.15)$ J/m^2. The adhesion energy γ_{adh} is defined by

$$\gamma_{adh} = \gamma_{001} - \gamma_i + \gamma_{STO} = \gamma_{001} - \gamma^*. \quad (3)$$

This results in $\gamma_{adh}=(3.05\pm0.15)$ J/m^2.

In summary, we have investigated Fe nanocrystal self-assembly on a $SrTiO_3(001)$-$c(4\times2)$ support. Our results show that iron crystallizes into a bcc structure, which results in truncated pyramid nanocrystal formation. A volume/shape analysis of these crystals shows that they have attained an equilibrium shape. Quantitative information on the effective surface energy has been derived from a detailed comparison between the observed shape of the nanocrystals and that resulting from a Wulff construction based on calculated surface energies. For bcc Fe on $SrTiO_3(001)$-$c(4\times2)$ we have obtained a value of the adhesion energy $\gamma_{adh}=(3.05\pm0.15)$ J/m^2. This system is a model template to study the size-dependent magnetic properties of self-assembled pyramidal Fe nanocrystals.

The authors would like to thank the Royal Society and DSTL for funding.

[1] A. Biedermann, M. Schmid, and P. Varga, Phys. Rev. Lett. **86**, 464 (2001).
[2] S. Muller, P. Bayer, C. Reischl, K. Heinz, B. Feldmann, H. Zillgen, and M. Wuttig, Phys. Rev. Lett. **74**, 765 (1995).
[3] J. Shen, C. Schmidthals, J. Woltersdorf, and J. Kirschner, Surf. Sci. **407**, 90 (1998).
[4] W. S. Lai and X. S. Zhao, Appl. Phys. Lett. **85**, 4340 (2004).
[5] Ch. Muller, H. Muhlbauer, T. Steffl, B. Rellinghaus, and G. Dumpich, J. Cryst. Growth **218**, 410 (2000).
[6] D. A. Muller, N. Nakagawa, A. Ohtomo, J. L. Grazul, and H. Y. Hwang, Nature (London) **430**, 657 (2004).
[7] F. Silly and M. R. Castell, Phys. Rev. Lett. **94**, 046103 (2005).
[8] M. R. Castell, Surf. Sci. **505**, 1 (2002).
[9] T. Kubo and H. Nozoye, Surf. Sci. **542**, 177 (2003).
[10] M. R. Castell, Surf. Sci. **516**, 33 (2002).
[11] G. Medeiros-Ribeiro, A. M. Bratkovski, T. I. Kamins, D. A. A. Ohlberg, and R. Stanley Williams, Science **279**, 353 (1998).
[12] F. M. Ross, J. Tersoff, and R. M. Tromp, Phys. Rev. Lett. **80**, 984 (1998).
[13] M. J. S. Spencer, A. Hung, I. K. Snook, and I. Yarovsky, Surf. Sci. **513**, 389 (2002).
[14] W. L. Winterbottom, Acta Metall. **15**, 303 (1967).